Waves and solitons in complex plasmas

Céline Durniak[1], Dmitry Samsonov[1], Paul Harvey[1], Sergey Zhdanov[2], & Gregor Morfill[2]

[1] Department of Electrical Engineering and Electronics, The University of Liverpool, Brownlow Hill, Liverpool L69 3GJ, United Kingdom
[2] Max-Planck-Institut für Extraterrestrische Physik, D-85740 Garching, Germany.
celine.durniak@liv.ac.uk

Résumé. Les plasmas complexes (ou poussiéreux) sont des gaz ionisés contenant des microparticules chargées. Ils peuvent exister à l'état solide, liquide ou gazeux et être le siège de différents phénomènes dynamiques comme les solitons, les chocs, les cônes de Mach, les transferts thermiques par phonons,... Nous présentons une étude expérimentale et théorique concernant les solitons dans les plasmas complexes. Pour cela, nous analysons les modifications du milieu causées par la propagation des ondes, les propriétés des solitons longitudinaux ainsi que l'interaction entre solitons contrapropagatifs et l'influence de l'inhomogénéité du milieu sur la propagation des ondes. Nous mettons en évidence le retard sur la trajectoire de deux solitons lors de leur collision et l'amplification ("raidissement") des solitons se propageant dans un milieu dont la densité décroît.

Abstract. Complex (dusty) plasmas consist of micron sized microparticles immersed into ordinary ion-electron plasmas. They can exist in solid, liquid or gaseous states and exhibit a range of dynamic phenomena such as linear and nonlinear dust waves, solitons, shocks, Mach cones, heat transfer by phonons, flows, etc. We report on the experimental and numerical study of dissipative solitons in complex plasmas. We investigated the structural and dynamic changes of the lattice due to wave propagation, properties of compressional solitons, as well as interaction of counter-propagating solitons and the influence of the lattice inhomogeneity on the soliton propagation. It was found that the colliding solitons are delayed by their interaction and that the solitons propagating in a lattice with reducing number density exhibit an increase of amplitude (steepening).

1 Introduction

Complex or dusty plasmas are plasmas with added microparticles (or dust grains). The microparticles collect electrons and ions and become highly charged. Their charges are usually negative due to the higher mobility of electrons compared to ions and they are screened by the spatial rearrangement of the positive ions. The grains interact with each other electrostatically via a Yukawa (or Debye-Hückel, or screened Coulomb) potential.

Similar to colloids, complex plasmas can exist in solid, liquid or gaseous states and exhibit phase transitions [1]. If the Coulomb energy of two neighboring particles is larger than their thermal energy, they form ordered structures, which have liquid-like order. In cases of very low thermal energy compared to the potential energy of interaction, Coulomb solids are formed, which are often called "plasma crystals". Two-dimensional crystal lattices have a hexagonal structure. Complex plasmas are characterized by the screening parameter $\kappa = a/\lambda_D$, where λ_D is the Debye screening length and a is the interparticle spacing (usually of the order of $0.1 - 1$ mm).

Complex plasmas can be found in space, e.g. in planetary rings, comets or interstellar clouds. In plasma technology, dust contamination has negative effects on the yield of semiconductor devices. As the grains are weakly damped by gas friction and are traceable individually, dynamic phenomena such as shocks [2], Mach cones [3], solitons [4], and waves [5] can be observed at the kinetic level in real time.

Here we present the results of our experiments and molecular dynamics simulations of solitons in complex plasmas. The collision of two counter-propagating dissipative solitons was studied as well as the propagation of dissipative solitons in an inhomogeneous lattice.

2 Experimental setup

The experiments were performed in a capacitively coupled radio-frequency (rf) discharge chamber as shown in Fig. 1. Argon flow of either 3 sccm (collision experiment) or 1.2 sccm (steepening experiment) maintained the working gas pressure in the chamber of 1.446 Pa or 0.682 Pa respectively. The rf power of either 1 W (collision) or 2 W (steepening) was applied to the lower disc electrode which was 20 cm in diameter. The chamber itself was the other grounded electrode. Due to different area of the electrodes and different mobility of ions and electrons, the powered electrode had a DC self-bias voltage of 33 V (collision) or 35 V (steepening), which helped to suspend the particles in the plasma sheath against the gravity.

The particles that were injected into the plasma through a particle dispenser were monodisperse plastic microspheres of 9.19±0.1 μm in diameter with a mass m of 6.1×10^{-13} kg.

They were confined radially in a bowl shaped potential formed by a rim on the outer edge of the electrode, forming a monolayer hexagonal lattice of approximately 6 cm in diameter. The particles were illuminated by a horizontal thin (0.2-0.3 mm) sheet of light from a doubled Nd :YAG laser (532 nm) and imaged by a top-view digital camera at a rate of either 500 (collision) or 1000 (steepening) frames per second. Two parallel horizontal tungsten wires, both 0.1 mm in diameter were placed below the particle layer at 25.5 mm from the middle of the lower electrode. Both wires were normally grounded to minimize their influence on the particles. Short negative pulses with amplitudes between -10 and -40 V were applied to one or both wires to excite a single or two counter-propagating compressional disturbances respectively. A time interval of 100 s allowed the lattice to come to an equilibrium between the runs.

In order to analyze the experimental data, the positions of all particles were identified and they were traced in consecutive frames to calculate the particle velocities. The local two dimensional (2D) number density was determined as the inverse area of the Voronoi cells [6].

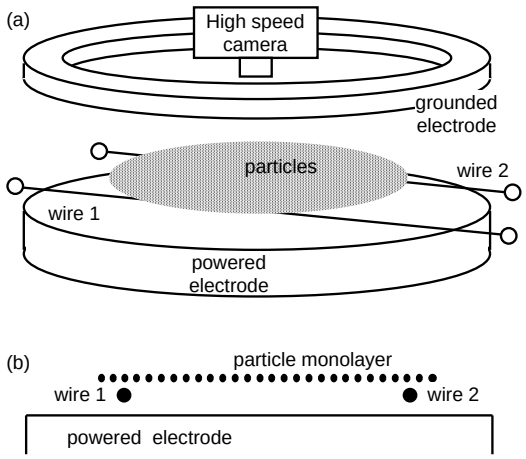

Fig. 1. Sketch of the apparatus. (a) Oblique view. Spherical monodisperse plastic microspheres charge negatively and form a monolayer levitating in the plasma sheath above the lower electrode. (b) Side view. Grounded wires are placed below the particles. Short negative voltage pulses are applied to the wires in order to excite solitons.

3 Molecular dynamics simulations

Using a three-dimensional (3D) molecular dynamics code, we simulated a monolayer complex plasma consisting of 3000 negatively charged microparticles interacting via a Yukawa potential. The code did

not include any explicit plasma. The plasma was taken into account only as the confining and interaction potentials. The 2D or 3D equations of motion were solved as follows :

$$\begin{aligned} m\ddot{\mathbf{r}}_s &= \mathbf{f}_s^{fr} + \mathbf{f}_s^{conf} + \mathbf{f}_s^{int} + \mathbf{f}_s^{ext} \\ \mathbf{f}_s^{fr} &= -m\nu\dot{\mathbf{r}}_s, \quad \mathbf{f}_s^{conf} = -m[\Omega_h^2(\mathbf{x}_s + \mathbf{y}_s) + \Omega_z^2\mathbf{z}_s] \\ \mathbf{f}_s^{int} &= -\nabla U_s, \quad U_s = Q^2 \sum_{j \neq s} r_{sj}^{-1} \exp(-r_{sj}/\lambda_D) \end{aligned} \tag{1}$$

where m is the mass of the particles, $\mathbf{r}$=$\mathbf{x}$+$\mathbf{y}$+$\mathbf{z}$ is the particle coordinate with the subscripts s and j denoting different particles, $\mathbf{f}_s^{fr}$ is the friction due to collisions with neutrals (Epstein or gas drag), $\mathbf{f}_s^{conf}$ is the confinement force due to the parabolic potential, $\mathbf{f}_s^{int}$ is the grain-grain interaction force, $\mathbf{f}_s^{ext}$ is the external excitation force, ν is the neutral damping rate, Ω_h and Ω_z are respectively the horizontal and vertical confinement parameters of the parabolic well, U_s is the Yukawa interaction potential, λ_D is the Debye screening length, Q is the particle charge, and $r_{sj} = |\mathbf{r}_s - \mathbf{r}_j|$ is the intergrain distance. The overdots denote time derivatives. The grain charge Q and the screening length λ_D were kept constant throughout the simulations.

The boundaries were free ; the grains were horizontally confined by a parabolic confining potential [7]. We used normalized units in the code : the lengths in terms of the screening length λ_D and the time in terms of $T = \sqrt{m\lambda_D^3/Q^2}$. In order to facilitate comparison to the experiment, the dimensionless units were converted into dimensional units after the simulation was completed.

Equations (1) were solved with the fifth order Cash Karp algorithm with adaptive step size controls [8]. We ran our simulations with the following parameters : $m = 5 \times 10^{-13}$ kg, $\nu = 1$ s^{-1}, $\lambda_D = 1$ mm, and $Q = 16000e$. Different values of the confinement parameter Ω_h enabled us to generate lattices with different screening parameters κ. We checked that the results of the 2D simulation matched those produced by the 3D code with $\Omega_z = 200$ Hz.

The particles were first placed randomly into the simulation box. Each particle then interacted with all the other particles and the code was run until the equilibrium was reached as the kinetic energy of the grains reduced (due to damping force chosen equal to the neutral friction force in the experiments) and a monolayer crystal lattice was formed. The lattice was then excited by a pulsed force applied inwards at either one or both sides of the lattice at a fraction of the lattice diameter from the center. The temporal shape was a truncated parabola with a duration of $\tau = 130$ ms (defined as the full width at half maximum amplitude of the pulse). The spatial profile in the x direction was either Gaussian or half-infinite with a Gaussian transition. It did not depend on the y coordinate (parallel to the soliton front).

In order to analyze the numerical data, the particle positions and velocities were recorded during the simulations. The 2D number density was determined from the Voronoi analysis similar to the analysis of the experiment.

4 Experimental and numerical results

4.1 Counter-propagating solitons

In order to study soliton collisions we obtained a homogeneous lattice which filled the space between the wires as shown in Fig. 1. Two identical compressional solitons were simultaneously excited to propagate inwards in the particle lattice. A brief negative potential lasting 100 ms was applied to both wires with an initial amplitude ranging between -20 V and -40 V.

Figure 2 shows a part of the lattice in the experiment with the propagating solitons before (a), during (b), and just after (c) the collision. As the solitons propagated inwards, their amplitudes decreased because of the neutral damping. Their evolution led to a collision in the middle of the lattice. At the point of collision the horizontal particle velocity (perpendicular to the wire) was zero. (Fig. 2 (b)). Then two waves emerged from the collision point. They were wider and had a reduced amplitude compared to the incident waves. Their centers were slightly retarded from the trajectories of the incoming centers by a *time delay* Δt. A similar effect has also been observed in hydrodynamics experiments [9].

The 3D simulation was performed with $\Omega_h = 0.5$ Hz, $\Omega_z = 50$ Hz. The excitation forces had identical Gaussian profiles along the x axis with a waist of 2 mm and an amplitude varying between 3 and 8 arbitrary units (arb. u.). They were applied at $\pm$ 1.7 cm from the center of the crystal, which was 9.25 cm in diameter.

The time delay Δt was determined from the "asymptotic" trajectories of the soliton maxima approximated as straight lines in (x, t) contour plots. Figure 3 shows that the time delay increases with the excitation amplitude in the experiments (a) and simulations (b).

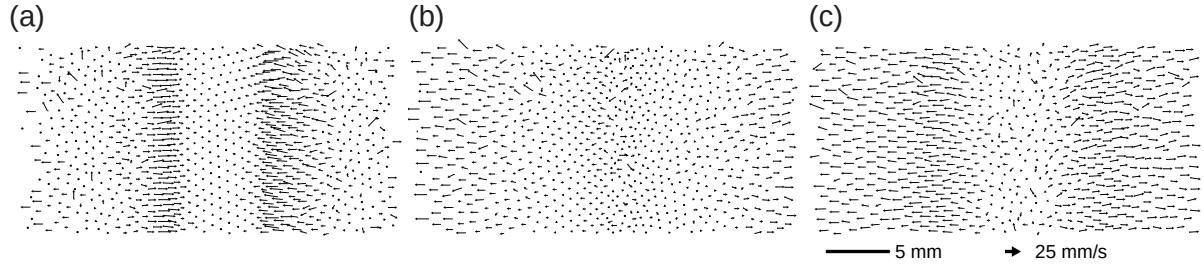

Fig. 2. Experimental particle velocity maps computed from two consecutive frames for an input pulse (-30 V) at t= 370 ms (a), 530 ms (b), and 690 ms (c).

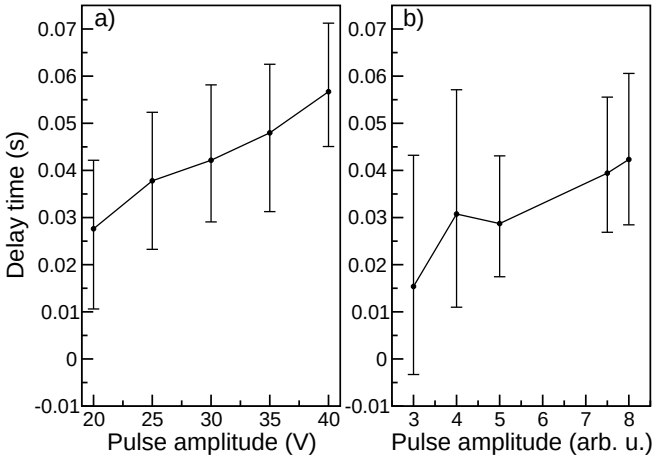

Fig. 3. Temporal delay of the interacting solitons measured from the particle velocity v_x versus excitation amplitude in the experiment (a) and the simulation (b).

4.2 Self-steepening effects

The soliton steepening was studied as it reached the inhomogeneous edge of the lattice. The experimental chamber was slightly tilted in order to maximize the lattice inhomogeneity on one side. Single solitons were excited in both the experiment and the simulation by either applying a voltage pulse to only one of the wires or an excitation force to one of the sides of the lattice. The spatial profile of the simulated excitation force was half-infinite in the x direction with a Gaussian transition [*i.e.* $\exp(-(x - x_0)^2/\omega^2)$ for $x \geq x_0$ and 1 for $x < x_0$] with $x_0 = -12$ mm and a waist ω of 2 mm. All the simulation runs were performed in 2D after verifying that the 3D simulation with $\Omega_z = 200$ Hz produced identical results.

Figure 4 shows the particle velocity v_x in the x direction. The snapshots of solitons were plotted at different times as they propagated along the x axis in the simulation (a) and in the experiment (b). The simulation of Fig. 4(a) was performed for the force amplitude $A = 1.5$ and screening parameter $\kappa = 0.725$ (determined in the middle of the lattice). In this crystal, the number density varied between 2.5 mm^{-2} at the center of the crystal to 0.75 mm^{-2} at the edge ($x_e = 23$ cm). The maximum of the particle velocity first decreased due to damping but then increased as the soliton reached the edge of the lattice where the number density decreased. We observed the same effect in the experiment (Fig. 4(b)) which was performed with a 5 s, -20 V excitation pulse.

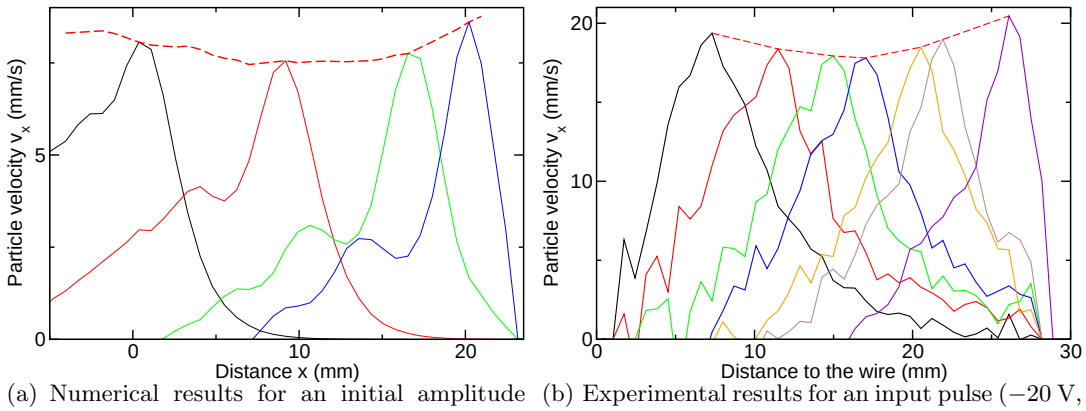

(a) Numerical results for an initial amplitude $A = 1.5$ and $\Omega_h = 2$ Hz at t=0.4 s, 0.6 s, 0.8 s, and 0.9 s.

(b) Experimental results for an input pulse (−20 V, 5 s) at t=398ms, 480ms, 553ms, 598ms, 681ms, 716ms, and 820ms.

Fig. 4. Particle velocity in the direction of the pulse propagation plotted versus distance to the excitation wire. Note that x is measured from the center of the crystal in the simulations and from wire 1 in the experiment.

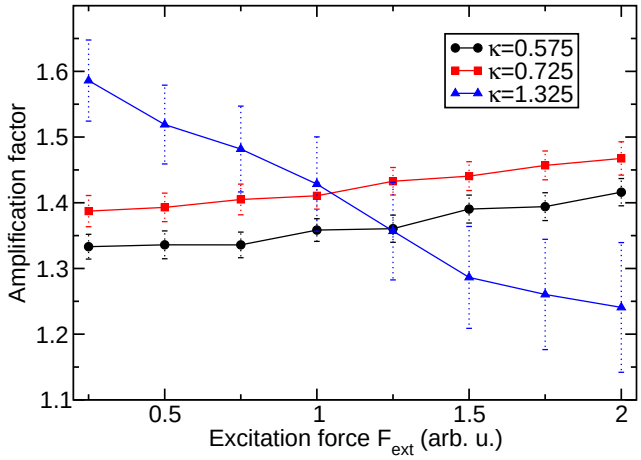

Fig. 5. Amplification factor of the pulse as a function of the initial amplitude of the excitation force A for different values of the screening parameter κ.

The influence of the excitation force amplitude A and the screening parameter κ was investigated numerically. Figure 5 shows the soliton amplification factor as a function of the excitation force amplitude

for different values of κ (ranging between 0.575 and 1.325). The amplification factor was calculated as the ratio of the final soliton amplitude to its amplitude in the middle of the lattice. In order to compare the runs with different κ we determined the final point as the point x_e where the number density decreased by a factor of 0.42 compared to its value in the center of the lattice. The damping rate was corrected for by multiplying the final amplitude by the factor $\exp(\nu(t_e - t_0)/2)$ where t_e and t_0 corresponded to the soliton at the $x = x_e$ and $x = 0$ positions respectively.

It was found that the amplification factor increases with the intensity of the excitation force at small κ but the effect is the opposite for the largest value of κ. This behavior requires explanation.

5 Conclusion

The properties of dissipative solitons propagating in complex plasmas were investigated experimentally and numerically. First, we analysed counter-propagating solitons and found that there is a time delay caused by their interaction. The time delay increased with the soliton amplitude. Second, we studied the soliton steepening as it propagated in a lattice with decreasing number density. The soliton amplification factor increased with the excitation amplitude at small values of the screening parameter. For the largest value of the screening parameter the amplification factor decreased with the excitation amplitude.

We thank the Engineering and Physical Sciences Research Council of the United Kingdom for financial support (grant EP/E04526X/1).

Références

1. H.M. Thomas and G.E. Morfill, Melting of a plasma crystal, *Nature*, **379**, 806-809 (1996) — C.A. Knapek, D. Samsonov, S. Zhdanov, U. Konopka, and G.E. Morfill, Recrystallization of a 2D plasma crystal, *Physical Review Letters*, **98**, 015004 (2007).
2. D. Samsonov, S.K. Zhdanov, R.A. Quinn, S.I. Popel, and G.E. Morfill, Shock melting of a two-dimensional complex plasma, *Physical Review Letters*, **92** (25), 255004 (2004).
3. D. Samsonov, J. Goree, H.M. Thomas, and G.E. Morfill, Mach cone shocks in a two-dimensional Yukawa solid using a complex plasma, *Physical Review E*, **61** (5), 5557-5572 (2000).
4. D. Samsonov, A.V. Ivlev, R.A. Quinn, G. Morfill, and S. Zhdanov , Dissipative longitudinal solitons in a two-dimensional strongly coupled complex (dusty) plasma, *Physical Review Letters*, **88** (9), 095004 (2002) — T.E. Sheridan, V. Nosenko, and J. Goree, Experimental study of nonlinear solitary waves in two-dimensional dusty plasma, *Physics of Plasmas*, **15**, 073703 (2008).
5. D. Samsonov, S. Zhdanov, and G. Morfill, Vertical wave packets in a crystallized hexagonal monolayer complex plasma, *Physical Review E*, **71**, 026410 (2005).
6. G.F. Voronoi, Nouvelles applications des paramètres continus à la théorie des formes quadratiques, Deuxième mémoire. Recherches sur les parallélоèdres primitifs — *J. Reine Angew. Math.* **134**, 198 (1908) and **136**, 67 (1909).
7. U. Konopka, L. Ratke, and H. M. Thomas, Central collisions of charged dust particles in a plasma, *Physical Review Letters*, **79**, 1269 (1997) — U. Konopka, G. E. Morfill, and L. Ratke, Measurement of the Interaction Potential of Microspheres in the Sheath of a rf Discharge, *Physical Review Letters*, **84**, 891 (2000).
8. W.H. Press, S.A. Teukolsky, W.T. Vetterling, and B.P. Flannery, *Numerical Recipes in C*, Cambridge University Press, New York, 2nd Edition (1992).
9. W. Craig, P. Guyenne, J. Hammack, D. Henderson, and C. Sulem, Solitary wave interactions, *Physics of Fluids*, **18**, 0571006 (2006) — A.B. Ezersky, O.E. Polukhina, J. Brossard, F. Marin, and I. Mutabazi, Spatiotemporal properties of solitons excited on the surface of shallow water in a hydrodynamic resonator, *Physics of Fluids*, **18**, 067104 (2006).